ELSEVIER

Chemical Engineering Journal 110 (2005) 67–78

Chemical Engineering Journal

www.elsevier.com/locate/cej

A general kinetic model framework for the interpretation of adiabatic calorimeter rate data

Arijit Bhattacharya *

Chemical Engineering and Process Development Division, National Chemical Laboratory, Pashan Road, Pune 411008, India

Received 6 May 2005; accepted 6 May 2005

Abstract

Notwithstanding the variety and complexity of the reactions studied by adiabatic calorimeters like ARC, the data interpretation techniques are not general enough. Traditional thermokinetic analysis primarily lumps a complex multi-step reaction into a single overall reaction and ignores possible thermal effects in some of the possible side reactions. With detailed chromatographic/mass spectrometric analysis of the headspace gases and the condensed phase residues, the pressure profile becomes an additional source of identification of the mechanism and the kinetics of the overall reaction. Finally, in the context of new multiphase catalytic processes of greater efficiency and environment friendliness and with reference to the storage of potentially incompatible fluid mixtures in metallic containers, ARC studies of heterogeneous reaction systems are becoming part of the mandatory safety evaluations. With a few additional measurements a proper kinetic interpretation of the ARC data on such systems seems possible. The paper presents a general model that was shown to be easily adaptable to a number of published reactions of various complexities referred to above. Standard thermal hazard characteristics like the onset temperature, adiabatic temperature rise, self-heat rate, time-to-maximum rate, pressure–temperature profile, etc. could be accurately calculated by the model and these compared closely with the experimental data. It is hoped that the model would be useful as a general-purpose tool for the interpretation of adiabatic calorimetric data for the purpose of process hazard assessment.

Keywords: Kinetic modeling; Runaway reactions; Accelerating rate calorimeters (ARC); Multi-step reactions; MOC (material of construction) incompatibility in storage

1. Introduction

In view of the increasing premium attached, rightly, to the safety of manufacture, transport, storage and processing of chemicals, hazard evaluations for the chemical processes have become extremely important. More often than not knowledge of chemistry and chemical engineering needs to be combined in a creative manner in order to describe the factors causing and/or influencing the course of an undesirable incident. One of the hazards of great concern to the chemical industry is the thermal runaway, which is governed by the thermodynamics and chemical kinetics of the usually complex chemical reactions taking place in the chemical system. An associated problem is that of uncontrolled pressurization of the system that may potentially breach the containment resulting in a nasty blow up and damages that should rather be prevented earlier than managed later.

Given the obvious exothermicity of the reactive systems, one would always like to have quantitative measures on the temperature and pressure rise and, more importantly, the accelerating heating and the pressurization rates once the runaway has appeared to have set in. Among many techniques (DSC, DTA, etc.) developed to provide direct or indirect measures of these quantities, one based on the adiabatic calorimetric principle was developed specifically for the thermal kinetic hazard evaluations. With this technique not only can the kinetic aspects of the temperature and pressure rise associated with chemical reactions be evaluated, but the heat of reaction can also be determined.

The general principle of an accelerating rate calorimeter (ARC) carrying out a homogeneous reaction was described

* Tel.: +91 20 25893 041; fax: +91 20 25893 041.
E-mail address: abhattacharya@che.ncl.res.in.

1385-8947/$ – see front matter © 2005 Elsevier B.V. All rights reserved.
doi:10.1016/j.cej.2005.05.003

Nomenclature

a'	specific interfacial area for solid–liquid mass transfer (m^{-1})
A	component participating in the reaction network
c_{vb}	specific heat of the bomb material (kJ/kg/°C)
c_{vs}	specific heat of the sample (kJ/kg/°C)
C	concentration of the liquid phase components (kmol/m^3)
D	diffusivity of the solid solute (m^2/s)
d_{PS}	mean particle size of the solid (m)
g	acceleration due to gravity (m/s^2)
Gr	Grashoff number, $g\rho d_{PS}^3(\rho_s - \rho)/\mu^2$
ΔH	heat of reaction (kJ/mol)
k_l	solid–liquid mass transfer coefficient (m/s)
m_b	mass of the bomb (kg)
m_s	mass of the sample (kg)
M	number of components
n_g	number of non-condensable components
n_G	moles of non-condensable components
n_v	number of vapourizable components
N	number of reactions
p_{gas}	total partial pressure of the non-condensable components (Pa)
p_T	headspace pressure (Pa)
p_{vap}	total partial pressure of the vapourizable components (Pa)
p_V	pure component vapour pressure (Pa)
r	rate of reaction (kmol/m^3/s)
R	universal gas constant
Sc	Schmidt number, $\mu/\rho/D$
Sh	Sherwood number, $k_l d_{PS}/D$
t	time (s or min)
T	temperature (°C or K)
V_g	gas volume (m^3)
V_l	liquid volume (m^3)
w_s	solid loading (kg)
x	mole fraction of the liquid component
$\overline{x}$	liquid mole fraction vector
y	mole fraction of the gaseous component
$\overline{y}$	gas mole fraction vector
z	compressibility factor

Greek letters

γ	activity coefficient
μ	liquid viscosity (Pa s)
ν	stoichiometric coefficient
ρ	liquid density (kg/m^3)
ρ_s	solid density (kg/m^3)
$\Delta\rho$	density difference (kg/m^3)
ϕ	thermal inertia
Φ	fugacity coefficient

Subscripts

i	reaction
j	component
ref	reference component
0	initial

Superscripts

s	saturation
i	interface

by Townsend and Tou [1], assuming a pseudo-*m*th order single step overall reaction, from which useful quantities like adiabatic temperature rise (ATR), heat of 'reaction' (overall single reaction), self-heat rate, time to maximum rate (TMR) could be calculated. ARC, using the measured temperature versus time profile and the user provided values for the sample mass and specific heat and the thermal inertia, reports the values of the above quantities for the test reaction in question. The authors demonstrated their methodology in the case of the thermal decomposition of Diazald and also obtained approximate values for the Arrhenius parameters for the reaction. Leung et al. [2] used the same methodology to interpret data obtained from a bench-scale adiabatic reactor developed under the AIChE Design Institute for Emergency Relief System (DIERS) program, conducting several reactions like thermal polymerization of styrene, di-*t*-butyl peroxide (DTBP) decomposition and base-catalysed phenol–formaldehyde reaction.

The thermo kinetic analysis mentioned above was at best an approximate one (especially for the TMR calculation) and not quite general. Thus the equations do not apply to cases where multiple reactions (in a competitive-consecutive reaction network) take place, such as in the case of the decomposition of polyacrylonitrile (PAN) in an acid medium [3]. Used extensively as a model system in ARC studies, decomposition of DTBP is known to proceed through a series of secondary elementary reactions involving free radicals, following the initial thermal decomposition of DTBP. The termination of the free radicals is usually significantly exothermic [4]. Even if the overall reaction rate is controlled (as in this case) by a particular bond-breaking reaction, the overall ('measured') heat of reaction can be explained only in terms of a detailed free-radical mechanism for the secondary reactions leading to different liquid and gaseous products. Moreover, the gaseous products and the more volatile among the liquid products would actually account for the possible rise in the headspace pressure during the reaction period (the pressure–temperature profile), which is normally recorded along with the temperature–time data in a standard ARC run.

Apart from the utility of the quantity, "pressurization rate", from the point of view of the relief settings, the pressure profile along with a proper characterization of the headspace

components at the end of an experiment can yield valuable information about the mechanism and the kinetics of the reaction. The thermo kinetic analysis underlying the ARC data interpretation normally does not attempt this (Leung et al. [2], being an exception, had shown how the head-pressure prediction could be done for the case of styrene polymerization).

Much of the traditional ARC studies were restricted to homogeneous liquid systems with the associated gas phase. However, in course of evaluating hazards involving heterogeneous reactive systems like aromatic nitration, adiabatic calorimetry (PHI-TECH) was used [5]. In a study of a rather freak runaway problem relating to the storage of a mixture of an otherwise perfectly compatible pair of liquids in galvanized steel drums [6], ARC as well as other small scale adiabatic reactors were used for conducting what can be termed as a solid dissolution accompanied by a liquid phase reaction. These applications considerably widen the scope of analysis of data from adiabatic reactors conducting a complex set of reactions in one or more phases that may involve inter-phase transport.

The above background provides a motivation for putting in place a more general-purpose mathematical model that can be used to interpret a variety of kinetic data routinely obtained in adiabatic calorimeters such as ARC. If complete characterization and composition analysis of the gas phase enclosed in the head space and the liquid and/or the solid residues at the end of the experimental run could be accomplished (see, for instance, Iizuka and Surianarayanan [7] in the case of DTBP decomposition) together with the measured pressure–temperature–time data, a possibility opens up for appropriate kinetic modeling of complex hazardous reactions occurring in ARC. Appropriate model-based identification of a reaction system will benefit the design and scale-up of larger scale reactors to conduct the reaction commercially.

In this paper we present, at first, a model for an adiabatic calorimeter with a generalized reaction network operating in a homogeneous medium, which we try to validate against published data like the measured temperature, self-heat rate, TMR, composition and pressure profiles in the context of known examples of runaway reactions carried out in laboratory test calorimeters by varied groups of researchers. Afterwards it would be shown that the model could be suitably extended to include inter-phase transport so that it could be used to predict the runaway characteristics for a typical liquid–solid reaction carried out in an ARC.

Unlike a commercial software like Batch-CAD that has been used earlier [7] to interpret adiabatic calorimeter data (no attempt was made to predict the headspace pressure in that work), which according to the authors themselves [7] does not make clear to the practitioners what is going on behind the screen during simulation (inside a black-box so to speak), the model presented here is transparent and is easier to implement using standard ODE packages which are more commonly accessible and are far less expensive.

2. Mathematical model for an adiabatic calorimeter

2.1. Model assumptions

- Batch, constant volume and adiabatic reactor operation.
- Constant physicochemical and thermodynamic properties.
- Homogeneous liquid phase irreversible reaction(s) with power law rate expressions constituting the reaction network.
- Liquid phase non-ideality, if present, considered in terms of activity coefficients (Wilson or UNIQUAC).
- Vapour phase non-ideality, when present, represented by an equation-of-state (EOS) model (SRK).

Ideally, variation of the physical properties with temperature should be considered. Unfortunately, however, for many of the complex compounds of interest key property values are not always available even at one temperature (usually at 25 °C), let alone their temperature dependence. If the appropriate data on the temperature effect are available these can be plugged into the model easily. Most decomposition reactions, particularly as they often generate gaseous products, are irreversible ones. Extension of the model to take care of any reversible reaction, if present within the reaction network and is important to consider, poses no additional difficulty. There may be some reservation about the use of the cited methods for calculating the activity coefficients at higher pressures, which is the norm in the present scenario. Our justification in using them at present is partly that for the systems considered the liquid phase non-ideality is not very significant and that these are among the most general-purpose predictive methods available for the purpose with a wealth of published data on the model parameters [8]. If the liquid phase non-ideality is, indeed, a serious issue in a given problem and these methods are found inadequate specific methods meant for high-pressure vapour–liquid equilibria may be tried out.

2.2. Model equations

Given M components involved in N linearly independent, elementary reactions, the solvent, if present, being the $(M+1)$th one, n_v the vapourizable and n_g the non-condensable components, with $(n_v + n_g) \leq M + 1$, the reaction network can be represented as

$$\sum_{j=1}^{M} \nu_{ij} A_j = 0 \tag{1}$$

ν_{ij} is the (i,j)th element of the stoichiometric coefficient matrix, referring to the jth component in the ith reaction step (−ve for a reactant species and +ve for a product species).

2.2.1. Component mass balances

The dynamic changes in the concentration of the components A_j are given by

$$\frac{dC_{A_j}}{dt} = \sum_{i=1}^{N} \frac{\nu_{ij}}{|\nu_{i,\text{ref}}|} r_{i,\text{ref}} \tag{2}$$

subject to the specified initial conditions ($t = 0$)

$$C_{A_j} = C_{A_{j0}} \tag{2a}$$

$r_{i,\text{ref}}$ returns the absolute value of the rate of reaction of the reference component in the ith elementary reaction step.

2.2.2. Heat balance

$$\frac{dT}{dt} = \frac{V_l \sum_{i=1}^{N} (\Delta H)_{i,\text{ref}} r_{i,\text{ref}}}{m_s c_{vs} \phi} \tag{3}$$

subject to the initial condition

$$T = T_0 \tag{3a}$$

$\Delta H_{i,\text{ref}}$ is the heat generated/absorbed by the ith reaction step (+ve for an exothermic and −ve for an endothermic reaction) per mole of the reference component. m_s is the ARC sample mass (inclusive of the solvent when present), V_l the volume and c_{vs} the constant volume specific heat of the sample. ϕ is the thermal inertia defined as

$$\phi = 1 + \frac{m_b c_{vb}}{m_s c_{vs}} \tag{4}$$

As $m_b c_{vb}$ (the calorimeter heat capacity) is reduced vis-à-vis $m_s c_{vs}$ (the sample heat capacity), ϕ would approach 1.0 (which is the adiabatic limit). For instance, in a study of the thermal decomposition of Diazald in an ARC, loading 1.01 g Diazald in 2.88 g of diethyl ether in a bomb that weighed 19.39 g, Townsend and Tou [1] calculated the thermal inertia to be 2.0 (assuming the specific heats of the sample and the Hasteloy C), the bomb material, as 2.093 and 0.4187 J/°C/g respectively. There are other studies in different apparatus where ϕ varied from as low a value as 1.05 [2] to as high as 7.0 [9].

2.2.3. Headspace pressure

$$p_{\text{vap}} = \sum_{j=1}^{n_v} \frac{\gamma_j(\bar{x}, T) p^s_{Vj}(T) x_j}{f_j(\bar{y}, p_T, T)} \tag{5}$$

$$p_{\text{gas}} = \left(\sum_{j=1}^{n_g} n_{Gj} \right) \frac{z(\bar{y}, p_T, T) RT}{V_g} \tag{6}$$

$$\sum_j x_j = 1.0 \tag{7}$$

$$\sum_j y_j = 1.0 \tag{8}$$

$$p_T = p_{\text{vap}} + p_{\text{gas}} \tag{9}$$

In Eqs. (5)–(9), γ represents the activity coefficient, f the fugacity coefficient, z the compressibility, x and y the liquid and the gas phase component mole fractions (the overbar meaning the mole fraction vector). n_{Gj} represents the moles of the non-condensable component(s). The superscript s indicates the saturation and subscript V vapour (e.g., p^s_{Vj} denoting the pure component vapour pressure of the jth component).

2.3. Solution procedure

Eqs. (2) and (3) are typically a set of coupled, highly non-linear and generally stiff ordinary differential equations (ODE) of the initial value type. Deriving a stable, general purpose and accurate numerical solution procedure for these equations in the event of extremely steep temperature gradients is a non-trivial problem. There are many commercially available packaged ODE solvers that can be used depending on the accessibility of a given code, availability of adequate documentation regarding the algorithm used, step-size control, error tolerance, etc. We have used in this work the IMSL code IVPAG with the Gear method (from Visual Numerics). The solution provides some of the most important characteristics of a runaway reaction system, namely, the adiabatic temperature rise, the temperature variation with time, the variation of the self-heat rate with the temperature (hence the maximum self-heat rate), the temperature at the maximum rate and the time-to-maximum rate (TMR). Simultaneously with the Eqs. (2) and (3), Eqs. (5)–(9) are used to calculate the headspace pressure profile from which the pressurization rate can also be calculated if desired. The complete calculations could be organized easily on a computer program to run on a desktop PC.

In order to be able to do the above calculations one is required to specify following data: the frequency factor, the activation energy and the heat of reaction for each of the reaction steps, the mass, the volume and the composition of the sample and its average specific heat. The thermal inertia is calculated using Eq. (4) from the knowledge of the mass of the bomb and the specific heat of the material of its construction. The vapour pressure–temperature correlations (or the Antoine parameters), the Wilson/UNIQUAC parameters for all the vapourizable components (the reactants, the solvent and the liquid products, if any) and the critical properties of all the components in the headspace will also have to be provided. In case specific (or proprietary) correlations to calculate the vapour pressures are available these should preferably be used.

On specifying an initial value for the sample temperature the equations can be integrated to simulate the usually steep temperature rise corresponding to the onset of the self-heating period observed in a typical ARC experiment. The integration is continued till well after the maximum in the self-heat rate occurs and the temperature reaches

the maximum plateau and remains stationary there. The difference between this latter value and the onset temperature is reported as the adiabatic temperature rise. From these calculations the temperature–time, self-heat rate versus temperature, TMR-onset temperature and the pressure–time plots are easily generated.

As it will be seen in course of the model applications to various systems, most of the input data about the reaction stoichiometry, thermodynamic and physicochemical properties, reactor details are generally either reported or can be estimated by standard estimation procedures. The reaction kinetic parameters, on the other hand, are best estimated by trying to fit the model predictions on the temperature–time profile or the self-heat rate against the measured data. If the model is a true description of the reality not only would the match between the predicted and the experimental characteristics be very good, but the estimates should be in reasonable range of values and also, for known reactions, be consistent with the values reported already in the literature. For such estimations, in the present work, we have used an optimization module based on Levenberg–Marquardt algorithm (BCLSJ) in the IMSL library from the VISUAL Numerics.

3. Validation of the model

At the outset one would like to standardize and authenticate the calculation model devised in this work by comparing the model predictions of certain quantities of interest with observed data using some known examples of experimental studies from the literature.

3.1. Decomposition of Diazald

Diazald (*N*-methyl-*N*-nitroso-*p*-toluene sulfonamide) is ubiquitous in organic synthesis. Reaction of Diazald dissolved in diethyl ether with a basic solution is employed in the generation of diazomethane. Though generally known to be stable at room temperature a sample of Diazald dissolved in diethyl ether stored for months was reported to have detonated spontaneously [10]. Townsend and Tou [1] made an ARC study of this reaction and used their simplified thermo kinetic analysis to estimate the Arrhenius parameters assuming a single irreversible gas-producing decomposition reaction of the form:

$$A_1\,(\mathrm{l}) \rightarrow A_2\,(\mathrm{l}) + 0.4A_3\,(\mathrm{g})$$

Some of the input data in order to apply the model developed in this work to this system were taken from the cited paper and are summarized in Table 1. Others required for the VLE and headspace pressure prediction have been taken from Reid et al. [11]. The elements of the stoichiometric coefficient matrix are −1, 1 and 0.4 respectively for the three components. Fig. 1 shows the predicted temperature–time profile and Fig. 2 the variation of the self-heat rate with temperature. In both cases the model calculations closely match with the experimental data.

Table 1
Input data for the ARC study of the thermal decomposition of Diazald in diethyl ether

Quantities	
Reactor volume (m^3)	9.0×10^{-6}
Sample mass (kg)	3.89×10^{-3}
Sample specific heat (kJ/g/°C)	2.093×10^{-3}
Thermal inertia	2.0
Heat of reaction (kJ/mol)	209.34
Activation energy (kJ/mol)	116.64
Frequency factor (min^{-1})	4.58×10^{14}
Reaction order	1.0

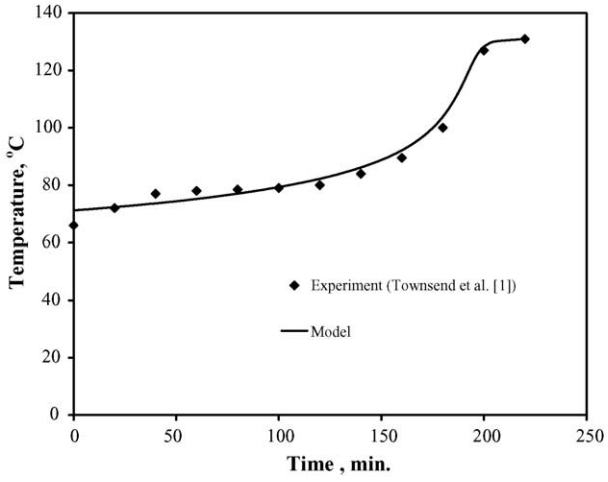

Fig. 1. Variation of the temperature with time for the thermal decomposition of Diazald in diethyl ether.

The quantities of interest in the process hazard analysis (PHA) calculated herein have been compared against the experimentally observed ones in Table 2. The last column of this table lists the corresponding quantities calculated by the simplified analysis [1]. As seen from this latter table, most

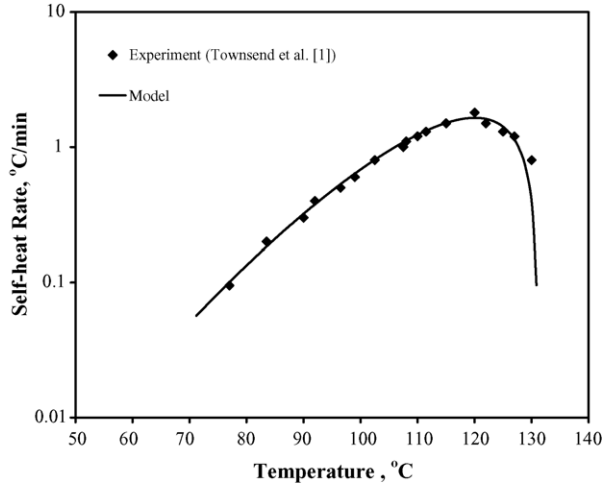

Fig. 2. Variation of the self-heat rate with temperature for the thermal decomposition of Diazald in diethyl ether.

Table 2
Comparison the observed and the predicted hazard characteristics in the ARC study of the thermal decomposition of Diazald in diethyl ether

Characteristics	Experiment [1]	Model (this work)	Simplified analysis [1]
Adiabatic temperature rise (°C)	60	59.9	60
Initial self-heat rate (°C/min)	0.044	0.0567	0.057
Maximum self-heat rate (°C/min)	1.8	1.647	1.7
Temperature at the maximum rate (°C)	120	119.89	120
Time-to-maximum rate (min)	199	192.5	143

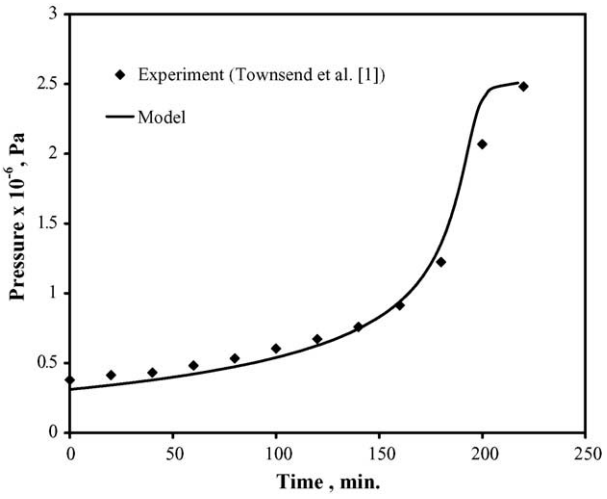

Fig. 3. Variation of the pressure with time for the thermal decomposition of Diazald in diethyl ether.

of the quantities have been predicted equally well by both the rigorous model and by the simplified analysis except for the TMR. This important characteristic is rather poorly calculated by the approximate formula whereas the present model gives a value much closer to the experimentally observed one.

Not only did the model predictions match closely the experimental observations on temperature, self-heat rate and the TMR (as well as or better than the approximate thermokinetic data interpretation methodology), but the headspace pressure was predicted simultaneously. In Fig. 3 the predicted pressure–time profile is also seen to come fairly close to the observed one. The approximate analysis was not equipped to predict the latter.

3.2. Decomposition of PAN in aqueous nitric acid solution

In the above example, though the overall decomposition may actually have been mediated through a complex mechanism, experimental data indicated that the observed rate is probably controlled by a single rate-controlling step and the runaway behaviour could be modeled well enough by a single overall reaction. However, there are published instances of complex reactions, which unfold through a series of competitive-consecutive steps each of which can be associated with a well defined reaction rate and may contribute to the overall heat generation. To demonstrate the generality and the validity of our model to a situation like this, we considered the observed runaway behaviour of the decomposition of an acrylic copolymer dissolved in nitric acid solutions (relevant in the industrial plants for the wet spinning of the copolymer from the acid liquors) for long hold-up times (~20–25 h). Analysis of the problem would be important in the context of the thermal runaway observed on many occasions with stored solutions after a fairly long hold-up period.

Arabito et al. [3] had studied the decomposition of a mixture of 92% polyacrylonitrile, 8% methylacrylate dissolved in a nitric acid–water solution taken in a Sikarex III adiabatic calorimeter and also suggested a four-step reaction network based on an initial hydrolysis of the cyanide groups followed by non-chain decomposition of the intermediates in a set of series and parallel reactions as follows:

$$\text{–CN} + \text{H}_2\text{O} \rightarrow \text{–CONH}_2 \quad \text{(a)}$$

$$\text{–CONH}_2 + \text{H}_2\text{O} + \text{H}^+ \rightarrow \text{–COOH} + \text{NH}_4{}^+ \quad \text{(b)}$$

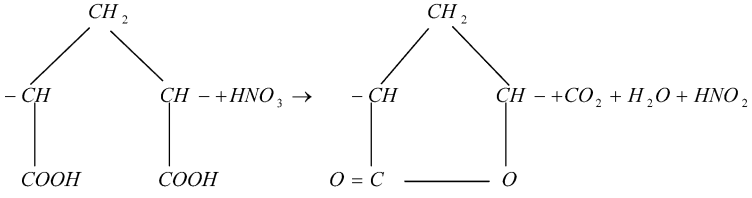

(c)

$$5\text{NH}_4\text{NO}_3 \rightarrow 4\text{N}_2 + 9\text{H}_2\text{O} + 2\text{HNO}_3 \quad \text{(d)}$$

The individual reactions involve component lumps characterized by functional end-groups such as, –CN, –CONH_2, –COOH and ions like $\text{NH}_4{}^+$ as well as the gaseous components like CO_2 and N_2. The reaction network was taken to be represented by the above four reactions, with their individual rates assumed to be first order in terms of the dissolved concentration of the pertinent end-groups. The relevant enthalpy of each of the reactions was taken from the same work [3]. The frequency factors and the activation energies were re-estimated in the present work to give the best fit with the experimental data on the variation of temperature and solu-

Table 3
Thermodynamic and the kinetic parameters for the reaction steps in the thermal decomposition of PAN in nitric acid solutions

Reaction	Enthalpy of reaction (kJ/mol)	Frequency factor (s^{-1})	Activation energy (kJ/mol)
1	87.923	1.0417×10^8	79.549
2	43.543	0.1389×10^8	75.362
3	82.899	7.5×10^4	66.989
4	246.184	361.11	46.055

tion composition with time [3] and, along with the heat of reaction data, have been summarized in Table 3. The head pressure was specifically calculated in this work based on the vapour pressure data for ∼69 wt.% nitric acid solution in water that forms an azeotropic composition corresponding to a temperature of 120 °C [19] and the non-condensable gases produced by the decomposition. The polymer loading was specified as 11 wt.%, its initial cyanide content as 0.052 mol and the onset temperature 30 °C. The thermal inertia was taken as unity so that the model would predict the temperature of the nitric acid–water solution under the true adiabatic conditions. Table 4 presents the stoichiometric coefficient matrix, specified for the calculation by the present model, whose elements ν_{ij} are as per the above reaction network.

Using the above information the model predicted correctly the adiabatic final temperature which is close to the azeotrope temperature, the maximum in the moles of –COOH end-group containing lump as 0.035 and that in the moles of NH_4^+ ions as 0.027, both of which are close to those experimentally observed [3]. Also the moles of the N_2 in the headspace would increase with time once the reactions get going reaching an asymptotic level (0.8 times the initial –CN moles) as observed experimentally. The calculated onset of the self-heating was around 20 h.

3.3. Decomposition of DTBP

The thermal decomposition of di-*t*-butyl peroxide (DTBP) has been one of the most extensively studied reactions [13–16] with a view to elucidating the details of the underlying free-radical mechanism. The overall reaction is supposed to follow a first-order (or near first-order) rate dependence on the DTBP concentration. This is also one of the most often used model reactions studied in ARC's by a number of groups (e.g., Smith et al. [9], Tou and Whiting [12], Leung et al. [2], Iizuka and Surianarayanan [7] to name a few). The reaction has been studied both with neat DTBP [7,9] and with DTBP dissolved in benzene [7], toluene [2,7,12], *t*-butyl benzene [14], isopropyl benzene [14], etc. as solvent. From all accounts, despite using different solvents (or no solvent at all) the activation energy calculated from the initial slope of the measured self-heat rate curve was found to be in the range of 151–163 kJ/mol. This observation suggests that despite possible variable contributions from different operative secondary radical reaction network in presence or absence of solvents, the breakage of the O–O bond in the peroxide to form two alkyloxo radicals is the rate-controlling step. On the other hand the importance of the specific reaction network (with an array of liquid and gaseous end products) cannot be exaggerated in respect of the contribution to the headspace pressure.

3.3.1. DTBP (dissolved in toluene)

For the purpose of further validating the model we considered the kinetic data [2] on DTBP decomposition in presence of toluene as a solvent obtained in a bench-scale adiabatic calorimeter (ARC). The calorimeter volume, the sample mass and its specific heat as well as the thermal inertia were reported [2] and taken as the input data in the model as shown in Table 5. Leung et al. [2] measured the heat of decomposition of DTBP as −177.5 kJ/mol (consistent with other independent measurements giving values in the range −167 to −188 kJ/mol). We have used this value in this work. From a careful review of the published kinetic data in the literature as well as the analysis of their own ARC data Smith et al. [9] recommended 0.925 as the reaction order for a pseudo-*m*th order single step overall decomposition of DTBP, which we have used here.

Fig. 4 presents a comparison of the model prediction of the self-heat rate versus temperature, an excellent fit that was used to estimate the activation energy and the frequency factor, the two kinetic parameters whose values appear in the last two rows of Table 5. Leung et al. [2] reported a value of 158.26 kJ/mol for the activation energy obtained graphically from the slope of the self-heat rate curve close to the onset temperature. Apart from the approximate nature of their estimation procedure, there are other reports of the value of the

Table 4
Stoichiometric coefficient matrix for the reaction steps in the thermal decomposition of PAN in nitric acid solutions

Reaction	Component						Reference component[a]
	1	2	3	4	5	6	
1	−1	1	0	0	0	0	–CN
2	0	−1	1	1	0	0	$-CONH_2$
3	0	0	−2	0	1	0	CO_2
4	0	0	0	−1	0	0.8	NH_4^+

[a] On which the rate is based.

Table 5
Input data for the ARC study of the thermal decomposition of di-*t*-butyl peroxide in toluene

Quantities	
Reactor volume (m^3)	0.12×10^{-3}
Sample mass (kg)	0.04
Sample specific heat (kJ/g/°C)	2.114×10^{-3}
Thermal inertia	1.11
Heat of reaction (kJ/mol)	177.52
Reaction order	0.925
Activation energy (kJ/mol)	151.19[a]
Frequency factor (s^{-1})	1.937×10^{15}[a]

[a] Estimated in this work.

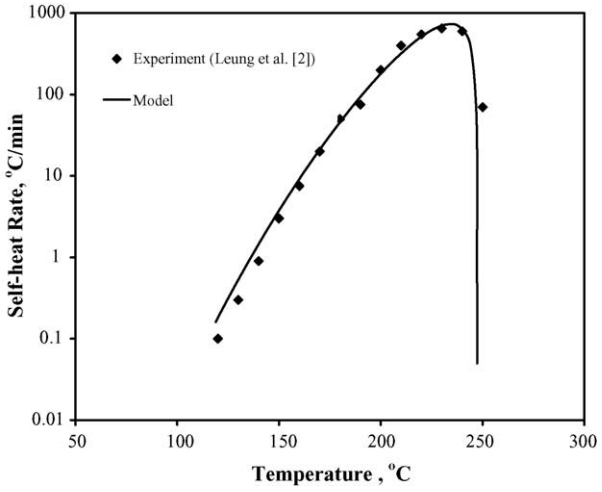

Fig. 4. Variation of the self-heat rate with temperature for the thermal decomposition of di-*t*-butyl peroxide in toluene.

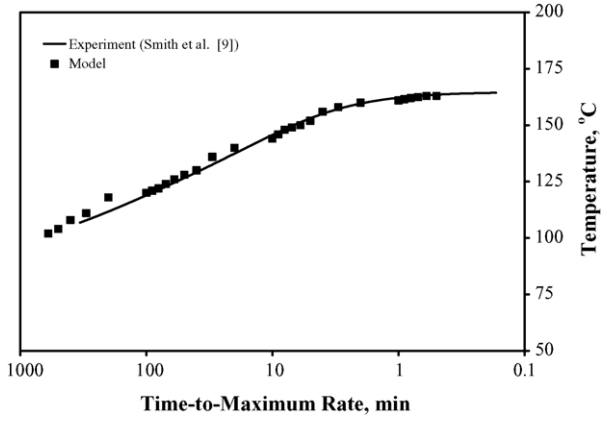

Fig. 5. Variation of the time-to-maximum rate with temperature for the decomposition of di-*t*-butyl peroxide (neat).

same quantity, namely, 150.72 kJ/mol [15] and 154.7 kJ/mol [7], which happen to be closer to the value used in this work that best fits the data.

3.3.2. DTBP (neat)

The performance of a Columbia Scientific Industries corporation (CSI) make ARC was characterized by Smith et al. [9] by studying the thermal decomposition of neat DTBP. The precision of the kinetic data was evaluated from 16 runs with a sample load of ∼2 g in a ∼70 g bomb giving a thermal inertia of about 7.0. Taking the same thermodynamic parameters (e.g., heat of reaction) as in Table 5 and an onset temperature of 106.8 °C the adiabatic temperature rise turned out to be 67.7 °C. Fig. 5 shows a fairly decent match of the model predicted variation of the TMR with temperature against

Table 6
Free-radical mechanism for the thermal decomposition of di-*t*-butyl peroxide in absence of any solvent

$(CH_3)_3COOC(CH_3)_3 \rightarrow 2(CH_3)_3CO^{\bullet}$

$(CH_3)_3CO^{\bullet} \rightarrow CH_3COCH_3 + CH_3^{\bullet}$

$(CH_3)_3COOC(CH_3)_3 + (CH_3)_3CO^{\bullet} \rightarrow (CH_3)_3COH + (CH_3)_3COOC(CH_3)_2CH_2^{\bullet}$

$(CH_3)_3COOC(CH_3)_3 + CH_3^{\bullet} \rightarrow CH_4 + (CH_3)_3COOC(CH_3)_2CH_2^{\bullet}$

$(CH_3)_3COOC(CH_3)_2CH_2 \rightarrow (CH_3)_2-C(O)-CH_2 + (CH_3)_3CO^{\cdot}$

$CH_3COCH_3 + CH_3^{\bullet} \rightarrow CH_3COCH_2^{\bullet} + CH_4$

$CH_3COCH_2^{\bullet} + CH_3^{\bullet} \rightarrow CH_3COCH_2CH_3$

$2CH_3^{\bullet} \rightarrow C_2H_6$

the experimentally measured profile as presented by these authors. The activation energy was slightly changed from the value as given in Table 5 to 152.82 along with a slight increase in the value of the pre-exponential factor (4.5×10^{15} in place of 1.94×10^{15}) for an improved match with this set of data.

The more interesting part was an attempt to predict the pressure–temperature profile experimentally determined by the same authors [9]. This called for a consideration of a reaction network as complete as practicable (consistent with the identification and analysis of the headspace species). Leung et al. [2] discussed in rudimentary and general manner some of the possible secondary reactions involving the initially generated butyloxo radicals [$(CH_3)_3CO^{\bullet}$] leading to gaseous products like ethane and vapourizable liquid products such as acetone and *t*-butyl alcohol.

Keeping in mind the various early reports on the mechanisms of decomposition of DTBP in the gas phase [15] and in various solvents [13,14,16] as well as a detailed study of thermal decomposition of cumene hydroperoxide [17] with a very similar product profile as in the case of DTBP, a consistent free radicals-based mechanism was independently derived in the present work and has been presented in Table 6 leading to the following overall reaction:

$$4(CH_3)_3COOC(CH_3)_3 \rightarrow 4CH_3COCH_3 + 2(CH_3)_2C(O)CH_2 + (CH_3)_3COH + CH_3COCH_2CH_3 + 2CH_4 + C_2H_6$$

It should be noted that this mechanistic pathway accounts for all the liquid and the gaseous product species, namely, acetone, *t*-butyl alcohol, isobutylene oxide, methyl ethyl ketone (MEK), methane and ethane as identified by Iizuka and Surianarayanan [7] through their product analysis (GC–MS). However, in the mechanism postulated by the latter authors the formation of MEK was associated with an unbalanced $H^{\bullet}$ radical (not explicitly shown in their mechanistic steps and also ignored in the overall stoichiometrically balanced reaction), which appears to be very unusual in the light of known decomposition mechanisms cited above. We found that the same overall stoichiometry could be obtained by invoking a different hydrogen abstraction step involving a methyl radical

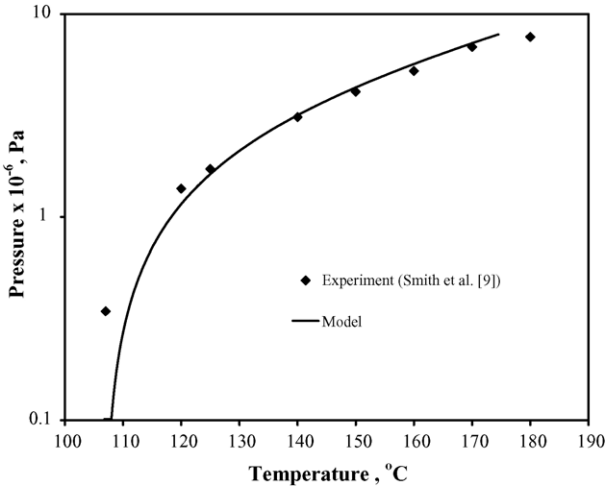

Fig. 6. Variation of the pressure with temperature for the thermal decomposition of di-*t*-butyl peroxide (neat).

already generated along with acetone. Each of the elementary steps in Table 6 as well as the overall reaction as shown above is balanced and the enthalpy change associated with each of these reaction steps can be calculated from the heat of formation data. From this the calculated enthalpy change for the overall reaction comes out as −160.5 kJ/mol which is close to some reported measured values.

Using the liquid and the gaseous product stoichiometric coefficients as per the overall reaction suggested above and choosing the UNIQUAC/SRK combination for predicting the vapour–liquid equilibria, the headspace pressure could be easily calculated by the model. The calculated headspace pressure versus temperature profile has been compared with the observed one in Fig. 6. The match is excellent considering the disparate source of the data and the postulated mechanism, lending an indirect support to the reaction network and also validating the calculation model proposed here.

4. Heterogeneous reactions in adiabatic calorimeter: extending the model applicability

The examples of the runaway reactions considered so far belong to the category of homogeneous ones. In the context of fine-chemicals manufacture there are occasions where thermal hazards may need to be considered in respect of reactions that are typically heterogeneously conducted.

An interesting thermal runaway hazard investigation was made by Wang et al. [6] in the context of the drum storage of a liquid mixture of thionyl chloride and ethyl acetate. There is no literature report of any potential reactivity hazard as to this particular mixture. However, storing the mixture in galvanized steel drums was found to initiate rupture of the vessels within less than an hour accompanied with the release of a cloud of noxious gas. The authors made systematic and detailed study of the causes underlying the thermal runaway by a number of bench tests of the compatibility of the mixture with the metals that form the material of construction (MOC) of the container drums. The finding squarely identified the dissolution of metallic zinc in the liquid mixture followed by a quick and exothermic gas-producing reaction in the liquid phase as the key runaway reaction responsible for the observed damage.

$$\mathrm{SOCl_2\,(l) + C_2H_5COOCH_3\,(l)} \xrightarrow{\mathrm{Zn\,(s)}} \mathrm{SO_2\,(g) + C_2H_5Cl\,(g) + CH_3COCl\,(l)}$$

In a series of carefully conducted experiments the heat generation characteristics of this reaction were measured in small scale adiabatic reactors holding the mixture and loading into it either drum scrapings, galvanized strips or fine zinc powder. On each occasion a runaway was invariably observed (after a small induction period) with variable heat generation and pressurization rates. Eventually the reaction was studied under a little more defined set of conditions in an ARC and the time–temperature profile and also various standard runaway characteristics were reported. We decided to try and simulate these results using the model presented in this paper.

4.1. Extended model

Strictly speaking the model as presented earlier is not directly applicable to this problem. The model formally needs a minor extension as to the inclusion of a solid–liquid mass transfer term in the component mass balance equation (2):

$$\frac{\mathrm{d}C_{A_j}}{\mathrm{d}t} = k_{\mathrm{l},A_j}a'(C^{\mathrm{i}}_{A_j} - C_{A_j}) + \sum_{i=1}^{N}\frac{\nu_{ij}}{|\nu_{i,\mathrm{ref}}|}r_{i,\mathrm{ref}} \tag{10}$$

In the above equations, the superscript i denotes interfacial value (of species concentration). For all components except the ones participating in the inter-phase transport the mass transfer coefficients (k_l) are set to zero.

In order to use the above equations, we need to specify both the specific surface area (a') and the mass transfer coefficient in an unambiguous manner, which is not easy in the present context. One is not sure whether stirring was provided in Wang et al.'s ARC experiment, and if so, if it was sufficient to suspend the loaded solid zinc strips as fully as possible (in all probability, it was not), nor about the exact solid loading. However, our purpose here goes beyond merely simulating a particular set of data and envisages applications (may be in the future) where such exothermic liquid–solid reactions would be studied in well-designed adiabatic calorimeters provided with appropriate stirring facilities and with known solid loading in a form that would allow the transport and the hydrodynamic parameters to be well defined. We therefore need to make some reasonable assumptions in order to attempt simulation of the already existing experimental results.

With the above proviso, the solid phase was assumed to be in a fine particulate form with a defined size cut or character-

ized by a mean particle size. In that case a' can be calculated as

$$a' = \frac{6w_s}{\rho_s d_{PS} V_l} \tag{11}$$

where w_s represents the solid loading, d_{PS} the mean particle size of the solid phase, ρ_s the solid density.

Correlations for calculating the mass transfer coefficients for solid–liquid mass transfer in an agitated liquid will not be applicable here. Steinberger and Treybal [18] had provided a correlation for slowly moving liquids past single spheres as well as through beds of pellets. Disregarding the contribution of the dynamic part (for very low particle Reynolds numbers in the case of a marginally stirred liquid in an ARC) the Sherwood number (*Sh*) is correlated with the Schmidt (*Sc*) and the Grashoff (*Gr*) numbers as

$$Sh = 2.0 + 0.569(GrSc)^{0.25}, \quad GrSc < 10^8 \tag{12}$$

where

$$Sh = \frac{k_l d_{PS}}{D} \tag{12a}$$

$$Sc = \frac{\mu}{\rho D} \tag{12b}$$

$$Gr = \frac{g\rho d_{PS}^3(\rho_s - \rho)}{\mu^2} \tag{12c}$$

Using estimated values of density (ρ), viscosity (μ) of the mixture (from the corresponding properties of thionyl chloride and ethyl acetate) in consistent units, the value of k_l can be calculated by the above correlation (a typical value under the assumed conditions was 5.51×10^{-4} m/s).

4.2. Model prediction

Sample volume and mass were reported by Wang et al. [6]. A single overall reaction as above was assumed. Sample specific heat was estimated based on the pure component values and the liquid composition. The enthalpy change associated with the above reaction was estimated and reported by the authors (we have verified the same by using Benson's group contribution method). The reaction was taken to be first order with respect to both thionyl chloride and ethyl acetate. For the purpose of the present simulation it was assumed that zinc powder in a narrow size cut (50–75 μm) was added to the liquid and the typical loading was 200 kg per cubic meter mixture containing 43% thionyl chloride and 57% ethyl acetate (same as used in one of the exploratory experiments in the same study using a small scale adiabatic reactor). The saturation concentration of zinc in the liquid mixture was taken in our calculation to be about 6.778 kg/m^3 based on a separate experiment cited in their study. All these input data have been summarized in Table 7.

The remaining three quantities (in the last three rows of Table 7) being unknown were estimated in the present work by fitting the adiabatic temperature–time profile calculated by our model with that observed by Wang et al.'s ARC experiment [6]. Fig. 7 compares the predicted time–temperature plot with the experimental data. The excellent fit under the assumed conditions clearly suggests that the model, the basic input data and the fitted parameters were appropriate. The estimated value of the thermal inertia as well as that for the Arrhenius parameters seem to be quite reasonable.

Table 8 provides a comparison of the standard runaway characteristics predicted by the model with those experimentally observed and tabulated by Wang et al. [6]. Most of

Table 7
Input data for the ARC study of the dissolution of metallic zinc powder in a liquid mixture of thionyl chloride (43%) and ethyl acetate (57%)

Quantities	
Liquid volume (m^3)	5.0×10^{-6}
Sample mass (kg)	5.5×10^{-3}
Sample specific heat (kJ/g/°C)	2.093×10^{-3}
Heat of reaction (kJ/mol)	125.6
Mean particle size of Zn powder (μm)	62.5
Zn loading (kg/m^3 mixture)	200
Onset temperature (°C)	26
Reaction orders	1.0
Activation energy (kJ/mol)	83.74[a]
Frequency factor	4.3×10^{16}[a]
Thermal inertia	1.88[a]

[a] Estimated in the present work.

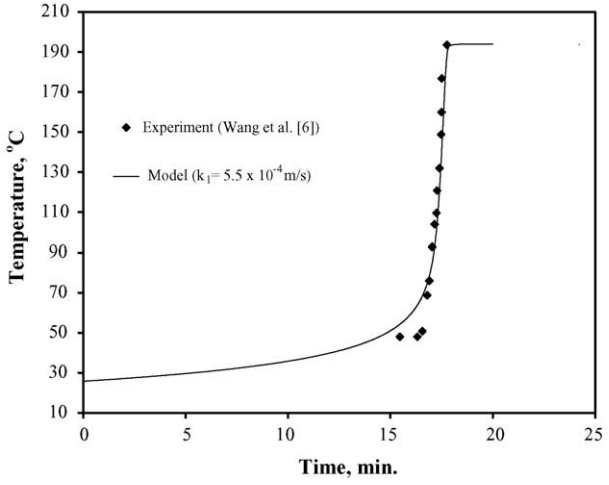

Fig. 7. Variation of the temperature with time for the runaway reaction between zinc and thionyl chloride–ethyl acetate mixture.

Table 8
Comparison the observed and the predicted hazard characteristics in the ARC study of the reactive dissolution of metallic zinc powder in a liquid mixture of thionyl chloride (43%) and ethyl acetate (57%)

Characteristics	Experiment [6]	Model (this work)
Final adiabatic temperature (°C)	193.1	193.7
Adiabatic temperature rise (°C)	167.1	167.7
Maximum self-heat rate (°C/min)	486.0	208.7
Temperature at the maximum rate (°C)	158.6	153.9
Time-to-maximum rate (min)	17.43	17.57

these have been predicted very well, except the value of the maximum self-heat rate. It must be remembered that the estimation of the derivative of the very steep time–temperature plot (especially the maximum) as obtained from ARC data analysis could sustain numerical errors if care is not taken, whereas the model calculates the derivatives with fairly high precision.

The point of the above exercise was not just that parameters could be found such that the model almost exactly reproduced the experimental ARC data in the case of a heterogeneous runaway reaction. A more important outcome probably is the hope that if such experiments could be planned more carefully in future and executed with an aim of interpreting data on a rational basis as shown here, the present model should be found quite useful as a data interpretation tool.

5. Conclusions

In this paper, a general mathematical model has been put in place that can be used to interpret a variety of kinetic data routinely obtained in adiabatic calorimeters such as ARC conducting runaway reactions. The generality is realized through a form of reaction network that can handle not only a simple overall reaction (if one truly occurs or if there is a single rate-controlling step) but more complex reaction networks as well. The latter may comprise of a series of (non-chain) competitive-consecutive reactions or may reflect multi-step free-radicals-based secondary chain reactions as in decomposition and oxidation reactions.

The model can be used to predict quantities of importance in hazard evaluation such as the onset temperature, the adiabatic temperature rise, the maximum self-heat rate, the temperature at the maximum rate, the time-to-maximum rate and the headspace pressure. If the characterization and composition analysis of the gas phase enclosed in the head-space and that of the liquid and/or the solid residues at the end of the experimental run in an ARC can be undertaken, together with the usual measurement of the pressure–temperature–time profiles, kinetic modeling of complex hazardous reactions occurring in the calorimeters should become feasible with the tools presented herein. This will enable a more informed approach to the design of larger scale reactors conducting this class of reactions.

As an indication of what could be accomplished, we have tried to show by systematically applying the general model to a number of reported examples of decomposition reactions (both single and multi-step complex ones) carried out in adiabatic calorimeters of varying characteristics by several researchers over a period of two decades. Not only was it possible to almost reproduce the observed time–temperature profiles (hence the self-heat rate and the TMR), but more interestingly, published data on the pressure–temperature profiles (such as in the case of the decomposition of DTBP) could be very closely simulated by the model in terms of a free-radical mechanism independently proposed in this work for the reaction.

Finally, it was shown that the measured characteristics obtained by carrying out a heterogeneous reaction (like the dissolution of a solid in a liquid mixture accompanied by an exothermic, gas-producing reaction) in ARC, could be easily simulated by an extended version of the model. Applications such as this may, however, call for a few additional measurements and possibly improved calorimeter designs. Apart from studying liquid–solid reactions of interest in the fine-chemicals manufacture, this approach may also be of use in analyzing potential runaway characteristics in problems related to the storage of reactive chemicals in containers with incompatible materials of construction.

Acknowledgements

The author is grateful to Dr. K.V. Raghavan, former Director, Indian Institute of Chemical Technology, Hyderabad, India, for his interest in the work presented here and the interesting and stimulating discussions the author had with him during the early part of this work.

References

[1] D.I. Townsend, J.C. Tou, Thermal hazard evaluation by an accelerating rate calorimeter, Thermochim. Acta 37 (1980) 1–30.
[2] J.C. Leung, H.K. Fauske, H.G. Fisher, Thermal runaway reactions in a low thermal inertia apparatus, Thermochim. Acta 104 (1986) 13–29.
[3] G. Arabito, V. Caprio, S. Crescitelli, G. Russo, V. Tufano, Runaway reactions in a polyacrylonitrile wet-spinning plant, Inst. Chem. Eng. Symp. Ser. No. 82 (1983) B10–B17.
[4] C.H. Bamford, C.F.H. Tipper (Eds.), Comprehensive Chemical Kinetics, vol. 16: Liquid Phase Oxidation, Elsevier, Amsterdam, 1980, p. 58.
[5] J.M. Zaldivar, C. Barcons, H. Hernandez, E. Molga, T.J. Snee, Modeling and optimization of semi-batch toluene mononitration with mixed acid from performance and safety viewpoints, Chem. Eng. Sci. 47 (1992) 2517–2522.
[6] S.S.Y. Wang, S. Kiang, W. Merkl, Investigation of a thermal runaway hazard drum storage of thionyl chloride/ethyl acetate mixture, Proc. Safety Prog. 13 (1994) 153–158.
[7] Y. Iizuka, M. Surianarayanan, Comprehensive kinetic model for adiabatic decomposition of di-*tert*-butyl peroxide using Batch CAD, Ind. Eng. Chem. Res. 42 (2003) 2987–2995.
[8] A. Fredenslund, J. Gmehling, P. Rasmussen, Vapour–Liquid Equilibria using UNIFAC, Elsevier, Amsterdam, 1977, pp. 21–26.
[9] D.W. Smith, M.C. Taylor, R. Young, T. Stephens, Accelerating rate calorimetry, Am. Lab. (Fairfield, Conn.) 12 (1980), 51–54, 56, 61–64, 66.
[10] Ref. [24] as quoted in [1] above.
[11] R. Reid, J.M. Prausnitz, T.K. Sherwood, The Properties of Gases and Liquids, 3rd ed., McGraw-Hill, New York, 1977.
[12] J.C. Tou, L.F. Whiting, The thermokinetic performance of an accelerating rate calorimeter, Thermochim. Acta 48 (1981) 21–42.
[13] E. Bell, F. Rust, W. Vaughan, Decompositions of di-*t*-alkyl peroxides. IV. Decomposition of pure liquid peroxide, J. Am. Chem. Soc. 72 (1950) 337–338.

[14] J. Raley, F. Rust, W. Vaughan, Decompositions of di-*t*-alkyl peroxides. III. Kinetics in liquid phase, J. Am. Chem. Soc. 70 (1948) 1336–1338.
[15] J. Murawski, J. Roberts, M. Szward, Kinetics of thermal decomposition of di-*t*-butyl peroxide, J. Chem. Phys. 19 (1951) 698–704.
[16] A.L. Williams, E.A. Oberright, J.W. Brooks, The abstraction of hydrogen atoms from liquid hydrocarbons by *t*-butoxy radicals, J. Am. Chem. Soc. 78 (1956) 1190–1193.
[17] M.S. Kharasch, A. Fono, W. Nudenberg, The chemistry of hydroperoxides. VI. The thermal decomposition of α-cumyl hydroperoxide, J. Org. Chem. 16 (1951) 113–127.
[18] R.L. Steinberger, R.E. Treybal, Mass transfer from a solid solute sphere to flowing liquid stream, AIChE J. 6 (1960) 227–232.
[19] R.H. Perry, D.W. Green, J.O. Maloney (Eds.), Perry's Chemical Engineers' Handbook, 7th ed., McGraw-Hill, New York, 1997, pp. 2–84.